# Antivitamins B<sub>12</sub> in a Microdrop: The Excited State Structure of a Precious Sample Using Transient Polarized X-ray Absorption Near Edge Structure

Nicholas A. Miller,<sup>1</sup> Lindsay B. Michocki,<sup>1</sup> Roberto Alonso-Mori,<sup>2</sup> Alexander Britz,<sup>2,3</sup> Aniruddha Deb,<sup>1,4</sup> Daniel P. DePonte,<sup>2</sup> James M. Glownia,<sup>2</sup> April K. Kaneshiro,<sup>5</sup> Christoph Kieninger,<sup>6</sup> Jake Koralek,<sup>2</sup> Joseph H. Meadows,<sup>1</sup> Tim B. van Driel,<sup>2</sup> Bernhard Kräutler,<sup>6</sup> Kevin J. Kubarych,<sup>1,4</sup> James E. Penner-Hahn,<sup>1,4\*</sup> and Roseanne J. Sension<sup>1,4,7\*</sup>

<sup>1</sup>Department of Chemistry, University of Michigan, 930 N University Ave. Ann Arbor, Michigan, 48109-1055, U.S.A.

<sup>2</sup>Linac Coherent Light Source, SLAC National Accelerator Laboratory, 2575 Sand Hill Road, Menlo Park, CA 94025, U.S.A.

<sup>3</sup>Stanford PULSE Institute, SLAC National Accelerator Laboratory, 2575 Sand Hill Road, Menlo Park, CA 94025, U.S.A

<sup>4</sup>Biophysics, University of Michigan, 930 N University Ave. Ann Arbor, Michigan, 48109-1055, U.S.A. <sup>5</sup>Department of Biological Chemistry, 1150 W. Medical Center Dr., Ann Arbor, Michigan, 48109-0600, U.S.A.

<sup>6</sup>Institute of Organic Chemistry & Center for Molecular Biosciences, University of Innsbruck, Innrain 80/82, A-6020 Innsbruck, Austria

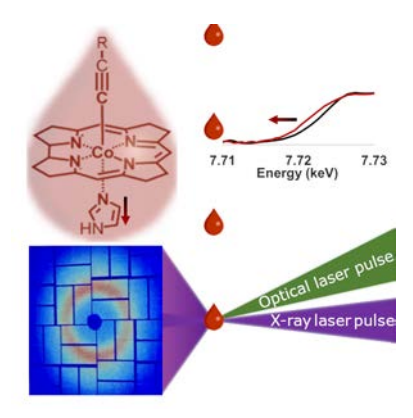
<sup>7</sup>Department of Physics, University of Michigan, 450 Church Street, Ann Arbor, Michigan, 48109-1040, U.S.A.

<sup>\*</sup> Corresponding Authors: <a href="mailto:rsension@umich.edu">rsension@umich.edu</a>, 734-763-6074, <a href="mailto:jeph@umich.edu">jeph@umich.edu</a>, 734-764-7324

### **ABSTRACT**

Polarized transient X-ray absorption near edge structure (XANES) was used to probe the excited state structure of a photostable  $B_{12}$  antivitamin (Co $\beta$ -2-(2,4-difluorophenyl)-ethynylcobalamin,  $F_2$ PhEtyCbl). A drop-on-demand delivery system synchronized to the LCLS X-ray free electron laser pulses was implemented and used to measure the XANES difference spectrum 12 ps following excitation, exposing only ~45  $\mu$ L of sample. Unlike cyanocobalamin (CNCbl), where the Co-C bond expands 15 to 20%, the excited state of  $F_2$ PhEtyCbl is characterized by little change in the Co-C bond, suggesting that the acetylide linkage raises the barrier for expansion of the Co-C bond. In contrast, the lower axial Co-N<sub>DMB</sub> bond is elongated in the excited state of  $F_2$ PhEtyCbl by ca. 10% or more, comparable to the 10% elongation observed for Co-N<sub>DMB</sub> in CNCbl.

## **TOC GRAPHIC**



Antivitamins  $B_{12}$  are a class of robust structural  $B_{12}$  mimics that resist metabolic conversion into  $B_{12}$ -cofactors and are capable of inhibiting vitamin  $B_{12}$  activity. The antivitamins  $B_{12}$  were previously studied with UV-Visible transient absorbance spectroscopy. The phenylethynyl-cobalamin (PhEtyCbl, Figure 1) antivitamin is photostable with internal conversion to the ground state on a ca. 60 ps time scale. These measurements and subsequent TD-DFT calculations suggest internal conversion to the ground state involves significant elongation or dissociation of the Co-N<sub>DMB</sub> bond in the excited state accompanied by smaller changes in the Co-C bond. Though information about the excited state structure can be inferred through UV-Visible spectroscopy, the spectra are dominated by corrin  $\pi$ - $\pi$ \* transitions and provide only indirect insight into the axial structural changes. The rational design of photoswitchable antivitamins  $B_{12}$  will require a more complete understanding both of the structural evolution of antivitamins following excitation to the excited state and of the parameters that control excited state structure and reactivity. For this reason, we have used time-resolved X-ray spectroscopy to determine the structure of the photoexcited state of the antivitamin F<sub>2</sub>PhEtyCbl (see Figure 1).

Figure 1. Schematic diagram of  $F_2$ PhEtyCbl illustrating the coordinate system used to describe the experimental results (R = 2,4-difluorophenyl-ethynyl). The initial transition dipole excited at 520

nm is approximately along the x-axis. The lower axial bond is denoted Co- $N_{DMB}$  when the reference is to experimental data and the full cobalamin structure and Co- $N_{IM}$  when the reference is to simulations on the truncated structure.

TD-DFT calculations of the CNCbl S<sub>1</sub> excited state identify a single excited state minimum characterized by ca. 10% elongation of the lower Co-N<sub>IM</sub> axial bond and 15 to 20% elongation of the upper Co-C bond. In contrast, TD-DFT calculations of the optimized excited states of PhEtyCbl suggest that the S<sub>1</sub> state is characterized by two minima, one local minimum near the Franck-Condon region with contracted axial bonds and a second lower energy minimum with an elongated lower axial bond Co-N<sub>IM</sub> > 2.6 Å and little change in the Co-C bond. These minima are separated by a barrier of 22 kJ/mol (5.3 kcal/mol). The excited state probed in UV-visible transient absorption measurements is consistent with elongated axial bonds suggesting population of this second minimum within 1 ps. The UV-visible data alone, however, is insufficient to distinguish between elongation of the upper or lower axial bonds. The polarized X-ray absorption near edge structure (XANES) difference spectrum is ideally suited to probe the structure of this excited state.

Previous work on the ultrafast and picosecond XANES of other B<sub>12</sub> compounds has given a cobalt-eye view of cobalamin bonding, <sup>12-16</sup> and polarized XANES difference spectra allow examination of structural changes in a molecule-fixed framework, further refining the structure of the excited state. <sup>12-15</sup> Ultrafast measurements on cyanocobalamin (CNCbl) demonstrated a ballistic, slightly underdamped expansion of the axial cobalt-ligand bonds. <sup>12</sup> The structure of this excited state is in good agreement with recent TD-DFT calculations. <sup>10-13</sup> In contrast, our study of methylcobalamin (MeCbl) demonstrates that the excited state for this molecule is dominated by changes in the corrin ring rather than changes in the axial bonds. <sup>14</sup> The combination of theoretical calculations of the potential energy surfaces (PES), transient optical spectroscopy, and ultrafast X-

ray spectroscopy using state-of-the-art X-ray free electron lasers (XFELs), allows us to converge on a "molecular-snapshot" view of bond evolution in the excited state.

Here we report a transient XANES measurement on the antivitamin  $B_{12}$ ,  $Co\beta$ -2-(2,4-difluorophenyl)-ethynylcobalamin, abbreviated  $F_2$ PhEtyCbl (see Figure 1).  $F_2$ PhEtyCbl is a derivative of PhEtyCbl.<sup>1,7,17,18</sup> The optical transient absorption spectra are similar to those reported for PhEtyCbl (Figure 2). The molecule reaches the  $S_1$  state within 1 ps. Subsequent conformational relaxation is observed on a ca. 6.5 ps timescale characterized by a slight blue-shift of the visible  $\alpha\beta$ -band followed by recovery of the ground state on a 72 ps time scale. The  $\alpha\beta$ -band shifts from 551 nm in the ground state to ca. 480 nm in the excited state. The blue shift of the visible absorption band is similar to that observed for CNCbl, although the excited state spectrum is broader and weaker than that of CNCbl (See Figure S1).<sup>19-21</sup>

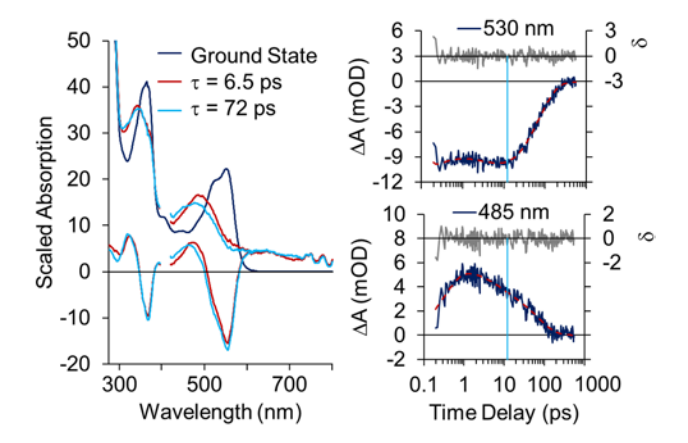


Figure 2. UV-visible transient absorption following excitation of F<sub>2</sub>PhEtyCbl at 400 nm. Left: the species associated difference spectra and estimated excited state spectra are compared with the ground state absorption spectrum. Right: kinetic traces (dark blue lines) at two probe wavelengths compared with the fit (red dashed lines) and the residuals (gray lines). The vertical light blue line indicates the time delay for the transient XANES measurement. See Figure S2 for a linear plot of the early time behavior.

Advances in spectroscopic sophistication are often accompanied by increased demands for sample availability. This is particularly true for photochemical reactions, since the techniques are inherently destructive. Sample availability places a severe limitation on our ability to study molecules such as the antivitamins, which are only available in relatively small quantities. Thus, sample management is a key technical challenge. For ultrafast X-ray experiments, the conventional liquid jet method (30 to 50 µm diameter) requires aqueous sample flow rates of 1-1.5 mL/min. 12,13,22-24 Recirculating a sample volume ≥ 10 mL is the only feasible way to maintain such flow rates. Unfortunately, mixing the exposed, and often contaminated, sample with the fresh reservoir can compromise the data unless the volume is large and/or changed frequently. In addition, interesting chemical systems like proteins, nucleic acids, bioconjugates, mimics, and exotic molecules like the antivitamins B<sub>12</sub>, are often difficult and/or expensive to synthesize and purify in large quantities. In order to realize fully the capabilities of devices such as X-ray free electron lasers, it is necessary to reduce the required sample volume. Ideally, an experiment will dispense the required sample for one laser shot then repeat. A microfluidic device, such as a microdispenser can deliver precise amounts of sample for each laser shot.<sup>25-28</sup> A drop-on-demand microdispenser delivery system synchronized to the LCLS X-ray free electron laser pulses was implemented and used to measure the XANES difference spectrum of 3.5 mM F<sub>2</sub>PhEtyCbl 12 ps after excitation. The micro-dispenser allowed characterization of the excited state structure requiring only ~90 picoliters per laser shot. At the LCLS repetition frequency of 120 Hz, this sample delivery method consumes 470 µL per 12-hour shift.

Parallel and perpendicularly polarized XANES difference spectra 12 ps after excitation of F<sub>2</sub>PhEtyCbl at 520 nm are plotted in Figure 3. The parallel and perpendicular difference spectra

are used to construct the isotropic XANES difference signal as  $\Delta I_{iso}=(\Delta I_{||}+2\Delta I_{\perp})/3$ . The isotropic difference signal is used to estimate the excited-state spectrum:

$$I_{Excited State} = \frac{\Delta I_{iso} + \alpha I_{Ground State}}{\alpha}$$

where  $\alpha$  is the excited fraction, I<sub>Excited State</sub> is the estimated excited state spectrum, and I<sub>Ground State</sub> is the laser-off ground state XANES spectrum. The estimated excited state spectrum for an excitation fraction of  $\alpha$ =0.2 is plotted in Figure 4(b) (See also Figure S3). From these plots, the XANES edge clearly shifts to lower energy. The red-shift of the XANES edge correlates with an increase in axial bond length consistent with the inferences based on the excited state UV-visible spectrum (Figure 2).

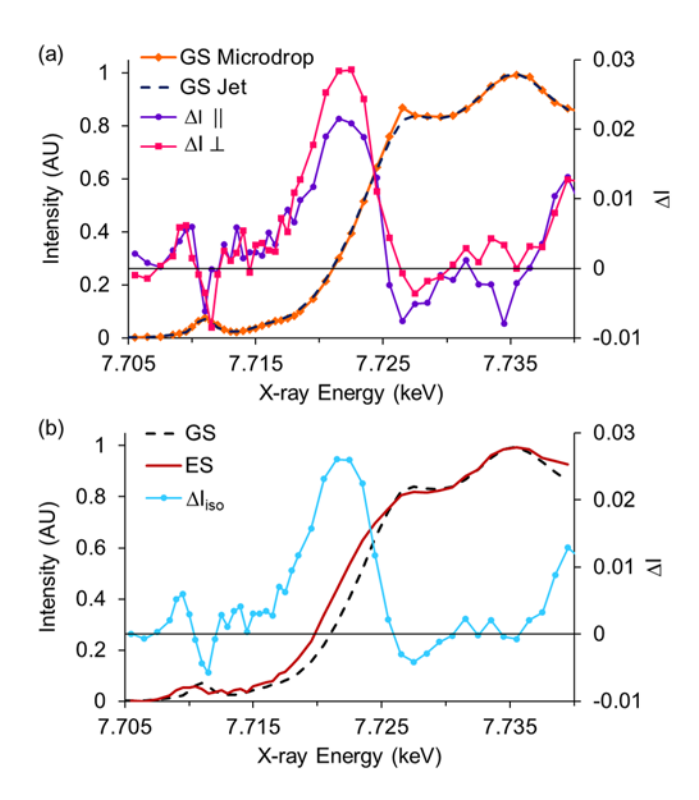


Figure 3. (a) Ground state XANES spectra of F<sub>2</sub>PhEtyCbl obtained using the microdropper and the liquid jet. The parallel and perpendicular difference spectra are plotted on the right-hand scale. The deviation between the two ground state spectra at 7.7265 keV is an artifact that cancels out in the

difference spectrum. (b) Isotropic XANES difference spectrum compared with the ground state XANES spectrum and the estimated excited state XANES spectrum.

Separation of the XANES difference signals into x- and y+z contributions provides more detail. A linear combination of parallel and perpendicular spectra creates molecule-fixed X-ray spectra. These x-polarized and y+z polarized difference spectra allow a taxonomic approach; classifying the major contribution of the x-polarized signal as equatorial ligands and y+z polarized signal as dominated by axial ligands.

$$\Delta I_x = 2\Delta I_{\parallel} - \Delta I_{\perp}$$

$$\Delta I_{y+z} = 3\Delta I_{\perp} - \Delta I_{\parallel}$$

The molecule-fixed difference spectra are shown in Figure 4 and compared with the molecule-fixed difference spectra for CNCbl in the  $S_1$  minimum (time delay > 600 fs)<sup>12</sup> and MeCbl in the  $S_1$  minimum at 100 ps.<sup>14</sup> See Figure S4 for a comparison of the isotropic difference spectra and the estimated excited state spectra. Both polarization components show a red-shift, characteristic of an elongation in the average bond length. The y+z-polarized amplitude is larger than the x-polarized amplitude. For  $F_2$ PhEtyCbl, the ratio of  $\Delta I_{y+z}$  to  $\Delta I_x$  is  $\sim$ 4.5:1. This is significantly smaller than for CNCbl ( $\sim$ 6.5:1) where axial bond elongation dominates, <sup>12,13</sup> but larger than for MeCbl ( $\sim$ 2:1) where axial and equatorial changes are comparable. <sup>14</sup> These comparisons indicate that the combined axial expansion is larger than the ring expansion in  $F_2$ PhEtyCbl, although smaller than the axial expansion in CNCbl. Comparison of the excited state X-ray absorption edge of  $F_2$ PhEtyCbl with the ground state of MeCbl suggests that the total axial expansion is ca. 0.2 Å (Figure S5). To quantify further the ligand expansion in  $F_2$ PhEtyCbl and to separate the contributions from the Co-C and Co-N<sub>DMB</sub> bonds, we performed FDMNES simulations of the X-ray cross-section. <sup>29,30</sup>

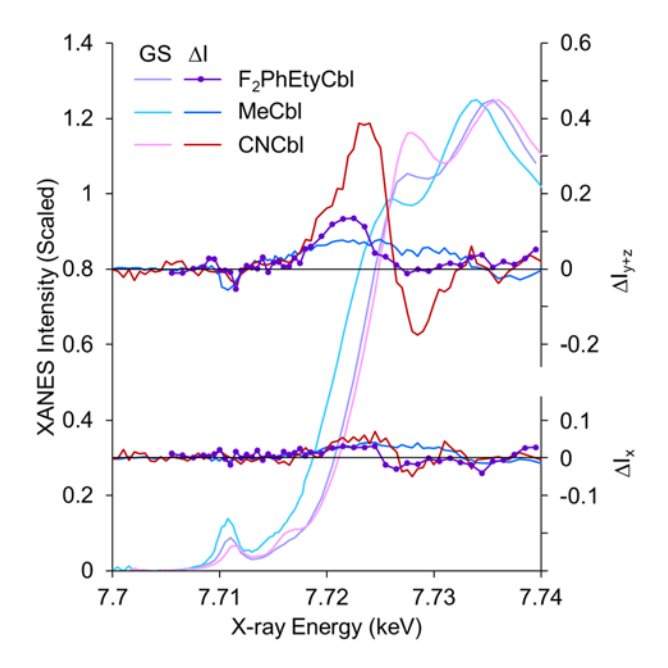


Figure 4. Decomposition of the XANES difference spectrum into contributions along the optically excited transition dipole in the corrin ring designated x and perpendicular to this direction, y+z. The data obtained for F<sub>2</sub>PhEtyCbl is compared with CNCbl in the S<sub>1</sub> minimum at time delays >600 fs<sup>12</sup> and MeCbl in the S<sub>1</sub> minimum at 100 ps. <sup>14</sup> The ground state XANES have been scaled to 1.25 at the high-energy peak for comparison. The difference spectra are on the same scale assuming the estimated excitation fraction for each measurement ( $\alpha$ =0.2 to 0.25).

Simulation of the XANES difference spectra begins with a truncated crystal structure for the ground state of PhEtyCbl (Figure 1) or a further truncation which replaces the phenyl group with a methyl group (MeEtyCbl).<sup>18</sup> See Supporting Information for more details. Ring expansion is modeled by using the crystal structure for the corrin ring in adenosylrhodibalamin (AdoRbl), which accommodates the much larger rhodium metal ion, and expanding by a set percentage along vectors connecting the atoms in the aligned AdoRbl and PhEtyCbl corrin rings.<sup>31</sup> This approximation avoids expansions of the corrin ring that are physically unrealistic. Changes in the axial bonds involve translation of the imidazole, PhEty, or MeEty groups along the z-direction.

An expansion of the full ring 25% to 30% between the ground state PhEtyCbl corrin ring and the AdoRbl ring is in qualitative agreement with the magnitude of the x-contribution to the difference spectrum (Figure 5a and S13). From this starting point, we made systematic changes in the axial bonds. An 0.09 Å expansion of the upper bond ( $\sim$ 5%) results in increased X-ray absorption in the region around 7.7255 keV without a significant shift of the XANES edge to lower energies (Figure 5b). Additional expansion results in an edge-shift to lower energies, but a simulated y+z difference spectrum that is significantly larger than the measured spectrum (see Figures S14 and S15 for additional examples).

Expansion of the lower bond by 0.2 Å to 0.3 Å (i.e. 9.6% to 14.4%) results in a shift of the XANES edge consistent with the observed difference spectrum (Figure 5c, S16). These expansions provide the best overall agreement with the measured difference spectrum. For comparison, contraction or expansion of the Co-C bond is combined with the Co-N<sub>IM</sub> expansion in Figure 5d. Although the qualitative trends are clear, a quantitative analysis of the structural changes upon excitation will require additional data (e.g., EXAFS) and perhaps the development of improved methods for modeling the XANES spectrum.

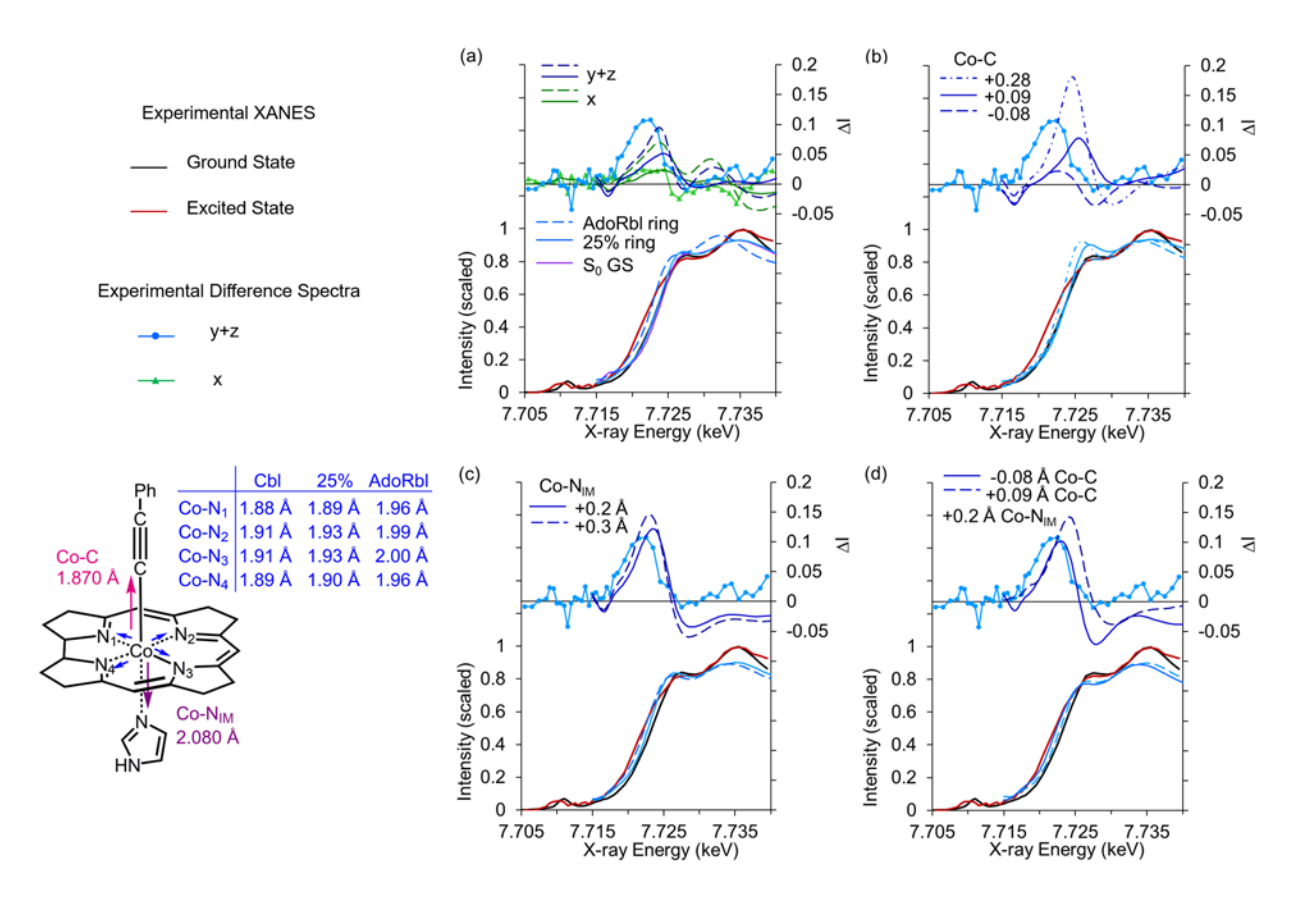


Figure 5. Comparison of experimental XANES data with simulations. The schematic at the left shows the ground state structure and the ring changes plotted. The legend for experimental data applies to panels a-d. (a) Influence of variations in the corrin ring on the excited state XANES and on the x and y+z difference spectra. The dashed lines are for the AdoRbl ring and the solid lines for the 25% expansion. (b) The influence of expansion or contraction of the Co-C bond on the excited state XANES and on the y+z difference spectrum. The 25% expansion is used for the ring. (c) The influence of expansion of the Co-N<sub>IM</sub> bond on the excited state XANES and on the y+z difference spectrum. The 25% expansion is used for the ring. (d) The combined influence of expansion of the Co-N<sub>IM</sub> bond accompanied by contraction or expansion of the Co-C bond on the excited state XANES and on the y+z difference spectrum. A 25% (dashed lines) or 30% (solid lines) expansion is used for the ring.

The XANES difference spectrum could be consistent with a modest contraction of the Co-C bond as predicted in recent TD-DFT calculations of the S<sub>1</sub> state of PhEtyCbl (ca. -0.085Å in TD-

DFT calculation). In contrast, the data show an expansion of the Co-N<sub>DMB</sub> bond while calculations predict that this bond is contracted in the local MLCT minimum. Thus, the excited state populated at 12 ps is not at the local MLCT S<sub>1</sub> minimum identified by TD-DFT calculations. Although the XANES spectra show a significant elongation of the Co-N<sub>DMB</sub> bond, they are not consistent with complete dissociation of this ligand to give a base-off cobalamin excited state. Thus, the excited state that is populated at 12 ps is also not the second, global, minimum identified in the calculations. The XANES difference spectra suggest the presence of a minimum on the excited state surface with a substantially elongated, but intact, lower bond. Internal conversion to the ground state requires barrier crossing from this region resulting in prompt return to the ground state, as no additional intermediates are observed in the optical measurements.

In attempting to understand the differences between our experimental structures and the theoretically predicted structures, it is important first to note that the TD-DFT calculations were performed on PhEtyCbl rather than F<sub>2</sub>PhEtyCbl and that they used a continuum approach, the conductor-like screening model (COSMO), to account for the effect of the solvent on the excited state. Our finding that the Co-N<sub>DMB</sub> bond is elongated but not broken could result from solvation interactions not included in the continuum approach, from the difference in the upper axial ligand, or from the influence of the full tethered dimethylbenzimidazole base in contrast to the imidazole used in the calculations. Notwithstanding these differences, both the calculations and the UV-visible and X-ray measurements suggest that internal conversion to the ground state occurs from an excited state that has an expanded Co-N<sub>DMB</sub> bond and a substantially unchanged Co-C bond. We note that the calculated barriers for escape from the local S<sub>1</sub> minimum of PhEtyCbl (ca. 22 kJ/mol) and escape from the global minimum (ca. 41 kJ/mol)<sup>8</sup> are both larger than the experimental barrier of ca. 13 kJ/mol that was found for this molecule.<sup>7</sup> This provides further evidence that the

TD-DFT calculations reproduce the excited state surface qualitatively, but only semiquantitatively.

The excited state produced following excitation of the photostable F<sub>2</sub>PhEtyCbl antivitamin B<sub>12</sub> is characterized by only modest changes in the Co-C bond length. In contrast, the Co-N<sub>DMB</sub> bond is elongated in the excited state, as much as 10 to 15% from ca. 2.080 Å to 2.280 Å or more. This is comparable to the 10% elongation observed for the lower bond in CNCbl (2.054 Å to 2.275 Å). That is, the primary difference between the excited state structures of CNCbl and F<sub>2</sub>PhEtyCbl is in the influence of photoexcitation on the Co-C bond length. This expands from ca. 1.85 Å in the ground state to ca. 2.20 Å in the excited state of CNCbl, while expanding very little, if at all, in F<sub>2</sub>PhEtyCbl. The acetylide linkage inhibits expansion and dissociation of the Co-C bond in the excited state in contrast to the photolabile Co-C bonds in alkylcobalamins.

In this work, we have also demonstrated the practical use of synchronized microdrop delivery for transient X-ray spectroscopy of precious samples, available only in small quantities. High quality polarized difference spectra were obtained within 70 minutes (i.e. ~5×10<sup>5</sup> pulses at 120 Hz, exposing ~45 μL of sample, corresponding to 0.16 μmoles or 0.23 mg of F<sub>2</sub>PhEtyCbl), despite the fact that the average hit rate was only ca. 50%. Improvements in the delivery system and the synchronization of the dropper will enable the investigation of a wide variety of precious photoactive samples in the future.

#### **EXPERIMENTAL METHODS**

XANES spectra were obtained for a room temperature solution of  $F_2$ PhEtyCbl using the XPP instrument of the XFEL LCLS at SLAC.<sup>32</sup> The X-ray pulses were focused to 25  $\mu$ m diameter at the sample. The femtosecond optical pump pulse was centered at 520 nm (10 nm full-width at half-maximum (FWHM)), with a focus of 150×220  $\mu$ m FWHM.<sup>33</sup> The sample was delivered as free-

space drops ~55 μm diameter with velocity 1 m/s. The X-ray and visible lasers intercepted drops 200 μm below the nozzle. A CSPAD detector was used to monitor the X-ray scattering from the drops and determine overlap of the X-ray beam with the drops. Analysis of the scatter signal allows for identification of missed drops and for correction for the effective volume of each drop that is illuminated. The average hit-rate for the measurements, that is, those cases where the sample drop was intercepted by the X-ray pulses, was ca. 50%. The transient spectra plotted in Figure 3 required about 70 minutes of beam time. A more dilute solution was also used in a liquid jet system to obtain a ground state XANES spectrum of F<sub>2</sub>PhEtyCbl. The ground state XANES from the drops and the liquid jet are consistent. UV-Visible transient absorption measurements were performed using a standard kHz Ti:Sapphire based system.<sup>7</sup> Additional experimental details are provided in Supporting Information.

#### **ACKNOWLEDGEMENTS**

This work was supported by grants from the National Science Foundation NSF-CHE 1464584, NSF-CHE 1836435 to RJS; NSF-CHE 1565795 to KJK. AKK was supported by NSF-CHE 1608553. Use of the Linac Coherent Light Source (LCLS), SLAC National Accelerator Laboratory, is supported by the U.S. Department of Energy, Office of Science, Office of Basic Energy Sciences under Contract No. DE-AC02-76SF00515.

#### SUPPORTING INFORMATION DESCRIPTION

Additional data figures, experimental and theoretical methods, comparison of the F<sub>2</sub>PhEtyCbl XANES difference spectrum with simulations.

#### REFERENCES

- (1) Ruetz, M.; Shanmuganathan, A.; Gherasim, C.; Karasik, A.; Salchner, R.; Kieninger, C.; Wurst, K.; Banerjee, R.; Koutmos, M.; Krautler, B. Antivitamin B<sub>12</sub> Inhibition of the Human B<sub>12</sub>-Processing Enzyme CblC: Crystal Structure of an Inactive Ternary Complex with Glutathione as the Cosubstrate. *Angew. Chem., Int. Ed.* **2017**, *56*, 7387-7392.
- (2) Brenig, C.; Ruetz, M.; Kieninger, C.; Wurst, K.; Krautler, B. Alpha- and Beta-Diastereoisomers of Phenylcobalamin from Cobalt-Arylation with Diphenyliodonium Chloride. *Chem. Eur. J.* **2017**, *23*, 9726-9731.
- (3) Ruetz, M.; Gherasim, C.; Gruber, K.; Fedosov, S.; Banerjee, R.; Kräutler, B. Access to Organometallic Arylcobaltcorrins through Radical Synthesis: 4-Ethylphenylcobalamin, a Potential "AntivitaminB12". *Angew. Chem., Int. Ed.* **2013**, *52*, 2606-2610.
- (4) Mutti, E.; Ruetz, M.; Birn, H.; Kräutler, B.; Nexo, E. 4-Ethylphenyl-Cobalamin Impairs Tissue Uptake of Vitamin B-12 and Causes Vitamin B-12 Deficiency in Mice. *PLoS One* **2013**, *8*, e75312.
- (5) Chrominski, M.; Lewalska, A.; Karczewski, M.; Gryko, D. Vitamin B-12 Derivatives for Orthogonal Functionalization. *J. Org. Chem.* **2014**, *79*, 7532-7542.
- Kräutler, B. Antivitamins B<sub>12</sub>-A Structure- and Reactivity-Based Concept. *Chem. Eur. J.* 2015, 21, 11280-11287.
- (7) Miller, N. A.; Wiley, T. E.; Spears, K. G.; Ruetz, M.; Kieninger, C.; Kräutler, B.; Sension, R. J. Toward the Design of Photoresponsive Conditional Antivitamins B<sub>12</sub>: A Transient Absorption Study of an Arylcobalamin and an Alkynylcobalamin. *J. Am. Chem. Soc.* **2016**, *138*, 14250-14256.
- (8) Lodowski, P.; Toda, M. J.; Ciura, K.; Jaworska, M.; Kozlowski, P. M. Photolytic Properties of Antivitamins B<sub>12</sub>. *Inorg. Chem.* **2018**, *57*, 7838-7850.

- (9) Lodowski, P.; Ciura, K.; Toda, M. J.; Jaworska, M.; Kozlowski, P. M. Photodissociation of Ethylphenylcobalamin Antivitamin B<sub>12</sub>. *Phys. Chem. Chem. Phys.* **2017**, *19*, 30310-30315.
- (10) Lodowski, P.; Jaworska, M.; Andruniów, T.; Garabato, B. D.; Kozlowski, P. M. Mechanism of the S<sub>1</sub> Excited State Internal Conversion in Vitamin B<sub>12</sub>. *Phys. Chem. Chem. Phys.* **2014**, *16*, 18675-18679.
- (11) Lodowski, P.; Jaworska, M.; Kornobis, K.; Andruniow, T.; Kozlowski, P. M. Electronic and Structural Properties of Low-Lying Excited States of Vitamin B12. *J. Phys. Chem. B* **2011**, *115*, 13304-13319.
- (12) Miller, N. A.; Deb, A.; Alonso-Mori, R.; Glownia, J. M.; Kiefer, L. M.; Konar, A.; Michocki, L. B.; Sikorski, M.; Sofferman, D. L.; Song, S.; et al. Ultrafast X-Ray Absorption Near Edge Structure Reveals Ballistic Excited State Structural Dynamics. *J. Phys. Chem. A* **2018**, *122*, 4963-4971.
- (13) Miller, N. A.; Deb, A.; Alonso-Mori, R.; Garabato, B. D.; Glownia, J. M.; Kiefer, L. M.; Koralek, J.; Sikorski, M.; Spears, K. G.; Wiley, T. E.; et al. Polarized XANES Monitors Femtosecond Structural Evolution of Photoexcited Vitamin B<sub>12</sub>. *J. Am. Chem. Soc.* **2017**, *139*, 1894-1899.
- (14) Michocki, L. B.; Miller, N. A.; Alonso-Mori, R.; Britz, A.; Deb, A.; Glownia, J. M.; Kaneshiro, A. K.; Konar, A.; Meadows, J. H.; Sofferman, D. L.; et al. Probing the Excited State of Methylcobalamin Using Polarized Time-Resolved X-ray Absorption Spectroscopy. *J. Phys. Chem. B* **2019**, *123*, 6042-6048.
- (15) Sension, R. J.; Miller, N. A.; Deb, A.; Alonso-Mori, R.; Glownia, J. M.; Penner-Hahn, J. E. Ballistic Excited State Dynamics Revealed by Polarized fs-XANES. *EPJ Web Conf.* **2019**, *205*, 05014.

- (16) Subramanian, G.; Zhang, X.; Kodis, G.; Kong, Q.; Liu, C.; Chizmeshya, A.; Weierstall, U.; Spence, J. Direct Structural and Chemical Characterization of the Photolytic Intermediates of Methylcobalamin Using Time-Resolved X-Ray Absorption Spectroscopy. *J. Phys. Chem. Lett.* **2018**, *9*, 1542-1546.
- (17) Ruetz, M.; Salchner, R.; Wurst, K.; Fedosov, S.; Kräutler, B. Phenylethynylcobalamin: A Light-Stable and Thermolysis-Resistant Organometallic Vitamin B<sub>12</sub> Derivative Prepared by Radical Synthesis. *Angew. Chem., Int. Ed.* **2013**, *52*, 11406-11409.
- (18) Chrominski, M.; Lewalska, A.; Gryko, D. Reduction-Free Synthesis of Stable Acetylide Cobalamins. *Chem. Comm.* **2013**, *49*, 11406-11408.
- (19) Wiley, T. E.; Arruda, B. C.; Miller, N. A.; Lenard, M.; Sension, R. J. Excited Electronic States and Internal Conversion in Cyanocobalamin. *Chin. Chem. Lett.* **2015**, *26*, 439-443.
- (20) Rury, A. S.; Wiley, T. E.; Sension, R. J. Energy Cascades, Excited State Dynamics, and Photochemistry in Cob(III)alamins and Ferric Porphyrins. *Acc. Chem. Res.* **2015**, *48*, 860-867.
- (21) Shiang, J. J.; Cole, A. G.; Sension, R. J.; Hang, K.; Weng, Y.; Trommel, J. S.; Marzilli, L. G.; Lian, T. Ultrafast Excited-State Dynamics in Vitamin B<sub>12</sub> and Related Cob(III)Alamins. *J. Am. Chem. Soc.* **2006**, *128*, 801-808.
- (22) Lemke, H. T.; Kjaer, K. S.; Hartsock, R.; van Driel, T. B.; Chollet, M.; Glownia, J. M.; Song, S.; Zhu, D. L.; Pace, E.; Matar, S. F.; et al. Coherent Structural Trapping Through Wave Packet Dispersion During Photoinduced Spin State Switching. *Nat. Commun.* **2017**, *8*, 15342.
- (23) Kjaer, K. S.; Kunnus, K.; Harlang, T. C. B.; Van Driel, T. B.; Ledbetter, K.; Hartsock, R. W.; Reinhard, M. E.; Koroidov, S.; Li, L.; Laursen, M. G.; et al. Solvent Control of Charge Transfer Excited State Relaxation Pathways in [Fe(2,2'-bipyridine)(CN)4]<sup>2-</sup>. *Phys. Chem. Chem. Phys.* **2018**, *20*, 4238-4249.

- (24) Shelby, M. L.; Lestrange, P. J.; Jackson, N. E.; Haldrup, K.; Mara, M. W.; Stickrath, A. B.; Zhu, D.; Lemke, H. T.; Chollet, M.; Hoffman, B. M.; et al. Ultrafast Excited State Relaxation of a Metalloporphyrin Revealed by Femtosecond X-Ray Absorption Spectroscopy. *J. Am. Chem. Soc.* **2016**, *138*, 8752-8764.
- (25) Verkouteren, R. M.; Verkouteren, J. R. Inkjet Metrology II: Resolved Effects of Ejection Frequency, Fluidic Pressure, and Droplet Number on Reproducible Drop-on-Demand Dispensing. *Langmuir* **2011**, *27*, 9644-9653.
- (26) Verkouteren, R. M.; Verkouteren, J. R. Inkjet Metrology: High-Accuracy Mass Measurements of Microdroplets Produced by a Drop-on-Demand Dispenser. *Anal. Chem.* **2009**, *81*, 8577-8584.
- (27) Dong, H. M.; Carr, W. W.; Morris, J. F. Visualization of Drop-on-Demand Inkjet: Drop Formation and Deposition. *Rev. Sci. Instrum.* **2006**, *77*, 085101.
- (28) Chatterjee, R.; Weninger, C.; Loukianov, A.; Gul, S.; Fuller, F. D.; Cheah, M. H.; Fransson, T.; Pham, C. C.; Nelson, S.; Song, S.; et al. XANES and EXAFS of Dilute Solutions of Transition Metals at XFELs. *J. Synchrotron Rad.* **2019**, *26*, DOI:10.1107/S1600577519007550.
- (29) Bunau, O.; Joly, Y. Self-Consistent Aspects of X-Ray Absorption Calculations. *J. Phys. Condens. Matter* **2009**, *21*, 345501.
- (30) Joly, Y. X-Ray Absorption Near-Edge Structure Calculations Beyond the Muffin-Tin Approximation. *Phys. Rev. B* **2001**, *63*, 125120.
- (31) Widner, F. J.; Lawrence, A. D.; Deery, E.; Heldt, D.; Frank, S.; Gruber, K.; Wurst, K.; Warren, M. J.; Krautler, B. Total Synthesis, Structure, and Biological Activity of Adenosylrhodibalamin, the Non-Natural Rhodium Homologue of Coenzyme B<sub>12</sub>. *Angew. Chem., Int. Ed.* **2016**, *55*, 11281-11286.

- (32) Chollet, M.; Alonso-Mori, R.; Cammarata, M.; Damiani, D.; Defever, J.; Delor, J. T.; Feng, Y. P.; Glownia, J. M.; Langton, J. B.; Nelson, S.; et al. The X-Ray Pump-Probe Instrument at the Linac Coherent Light Source. *J. Synchrotron Rad.* **2015**, *22*, 503-507.
- (33) Minitti, M. P.; Robinson, J. S.; Coffee, R. N.; Edstrom, S.; Gilevich, S.; Glownia, J. M.; Granados, E.; Hering, P.; Hoffmann, M. C.; Miahnahri, A.; et al. Optical Laser Systems at the Linac Coherent Light Source. *J. Synchrotron Rad.* **2015**, *22*, 526-531.